

Growth process and magnetic anisotropy of amorphous $\text{La}_x\text{Zn}_y\text{O}_z$ nanowire arrays

Fang-Kuo Wang, Xiao-You Yuan

School of Chemistry and Chemical Engineering, Anhui University, Hefei 230039, People's Republic of China
E-mail: yuanxy@ahu.edu.cn

Published in Micro & Nano Letters; Received on 13th January 2014; Accepted on 3rd March 2014

Amorphous $\text{La}_x\text{Zn}_y\text{O}_z$ nanowire arrays with average diameters of 90 nm have been fabricated by chemical co-precipitation under subatmospheric pressure suction filtration in porous anodic aluminium oxide template. The growth process of $\text{La}_x\text{Zn}_y\text{O}_z$ nanowire arrays was investigated through scanning electron microscopy, and the morphology, structure and components of the nanowire arrays were characterised by transmission electron microscopy, X-ray diffraction and energy dispersive X-ray spectroscopy. The room temperature hysteresis loops of $\text{La}_x\text{Zn}_y\text{O}_z$ nanowire arrays shows that the ratio of coercive force $H_c(\parallel)/H_c(\perp)$ achieved is about 13, and saturation magnetisation $M_s(\parallel)/M_s(\perp)$ is 1.3. The nanowire arrays possess obvious magnetic anisotropy arising from the shape anisotropy, and the easily magnetised direction is parallel to the axis of the nanowire arrays, which may determine potential applications on ultra-high-density magnetic memory material.

1. Introduction: Zinc oxide (ZnO) nanomaterials have been extensively investigated because of their applications for biosensors, photocatalysis, electrochemistry and magnetic memory [1–5]. One-dimensional ZnO nanostructures including nanorods, nanotubes and nanowires were synthesised by hydrothermal, sol-gel and electrodeposition owing to their promising properties [6–8].

Doping of rare earth ions into ZnO nanostructures could virtually enhance their performances. Khatamian *et al.* [9] discovered that the photocatalytic activity of La, Nd and Sm-doped ZnO nanoparticles in the degradation of 4-nitrophenol increases with Ln loading up to 4, 4 and 8 wt% and then decreases. La-doped ZnO nanoparticle, nanowires, nanoflowers and thin films were prepared by co-precipitation [10], solvothermal [11], ball milling [12], magnetron sputtering [13] and pneumatic spray pyrolysis [14]; their enhanced fluorescence, gas-sensing, transmittance, antibiosis and photocatalytic activity were obtained by the change of concentration of doping La, because La doping would increase the bandgap of ZnO, and reduce the density of oxygen vacancies. However, the contrary result was observed when ZnO was doped with transition metal, Young *et al.* [15] investigated the effect of dopants La, Cu on the magnetic properties of well-aligned ZnO nanowires arrays, and discovered that the ferromagnetism is restrained by Cu doping, but visibly enhanced by the La doping. Furthermore, to realise a target for applying nanostructures to the fields of subminiature devices, controllable synthesis of orderly aligned nanotube or nanowire arrays with large-scale and high length–diameter ratio is greatly desired.

In this Letter, we report amorphous $\text{La}_x\text{Zn}_y\text{O}_z$ nanowire arrays prepared by subatmospheric pressure suction filtration (SPSF) assisted chemical co-precipitation in the anodic aluminium oxide (AAO) template, and the growth process and magnetic anisotropic behaviour of nanowire arrays were investigated.

2. Experimental procedure: The AAO template (pores diameter of about 100 nm) was fixed on the subatmospheric pressure suction filtration device and the gas tightness was checked, then the 0.1 M NaOH solution and the mixed nitrate solution consisting of 0.01 M $\text{La}(\text{NO}_3)_3$ and 0.01 M $\text{Zn}(\text{NO}_3)_2$ were alternately flown into the nanopores of the AAO template under the action of subatmospheric pressure (about 0.01 MPa). This process was repeated several times until the solution could not pass through the nanopores of AAO. The total reaction time is about 60 min. Thus, the $\text{La}_x\text{Zn}_y(\text{OH})_n$ nanowire precursor was

formed by the successive precipitation reaction between 0.1 M NaOH and 0.01 M mixed nitrate solution in the AAO template, and the precursor was high-temperature decomposed into $\text{La}_x\text{Zn}_y\text{O}_z$ nanowire arrays at 400°C for 2 h. Then, to investigate the growth process of nanowire the SPSF-assisted successive co-precipitation total reaction time was decreased to 30 or 15 min, and the corresponding nanostructures were obtained by similar synthesis procedures.

Scanning electron microscopy (SEM; JSM-6700F) was employed to observe the morphological changes in the growth process of nanowire arrays, and transmission electron microscopy (TEM; H-800) and X-ray diffraction (XRD; MXP18AHF) with Cu K α were used to characterise the morphology, structure and chemical composition of the well-aligned $\text{La}_x\text{Zn}_y\text{O}_z$ nanowire arrays. The magnetic behaviour of the $\text{La}_x\text{Zn}_y\text{O}_z$ nanowire arrays was measured by a vibrating sample magnetometer (VSM; BHV-55), and the magnetic field was applied parallel or perpendicular to the axis of nanowire arrays, respectively. There was not any pretreatment for the $\text{La}_x\text{Zn}_y\text{O}_z$ nanowire arrays with the AAO template before the test of SEM, XRD and VSM, whereas the TEM test sample was prepared by etching of 1 M NaOH solution to completely eliminate the AAO template.

3. Results and discussion: The amorphous $\text{La}_x\text{Zn}_y\text{O}_z$ nanowire arrays have been successfully prepared by the technique of chemical co-precipitation combined with SPSF. SEM was used to characterise the surface morphology of the as-prepared nanostructure with the AAO template. Fig. 1 shows the SEM images of incomplete or well-aligned $\text{La}_x\text{Zn}_y\text{O}_z$ nanowire arrays produced from total reaction times of 15, 30 and 60 min, respectively. It can be seen from Fig. 1a that almost a half proportion of the test area is an empty template not filled by any nanoparticles, and the other half also could not grow nanowires completely. Fig. 1b shows that nanowires with a minor diameter have grown in the nanopores of the AAO template, leaving one-third of the nanopores' aperture vacant. Fig. 1c is the image of well-aligned nanowire arrays, the vast majority of nanopores in the AAO template are filled with complete nanowires to form perfect nanowire arrays with the AAO template, and the average diameter is 90 nm, consistent with the aperture of the AAO template. The TEM study was used for further characterisation of the morphology of $\text{La}_x\text{Zn}_y\text{O}_z$ nanowire arrays. Fig. 2 is a TEM image of $\text{La}_x\text{Zn}_y\text{O}_z$ nanowires, in which the length of nanowires is up to 1 μm ; a high-magnification nanowire is shown in the

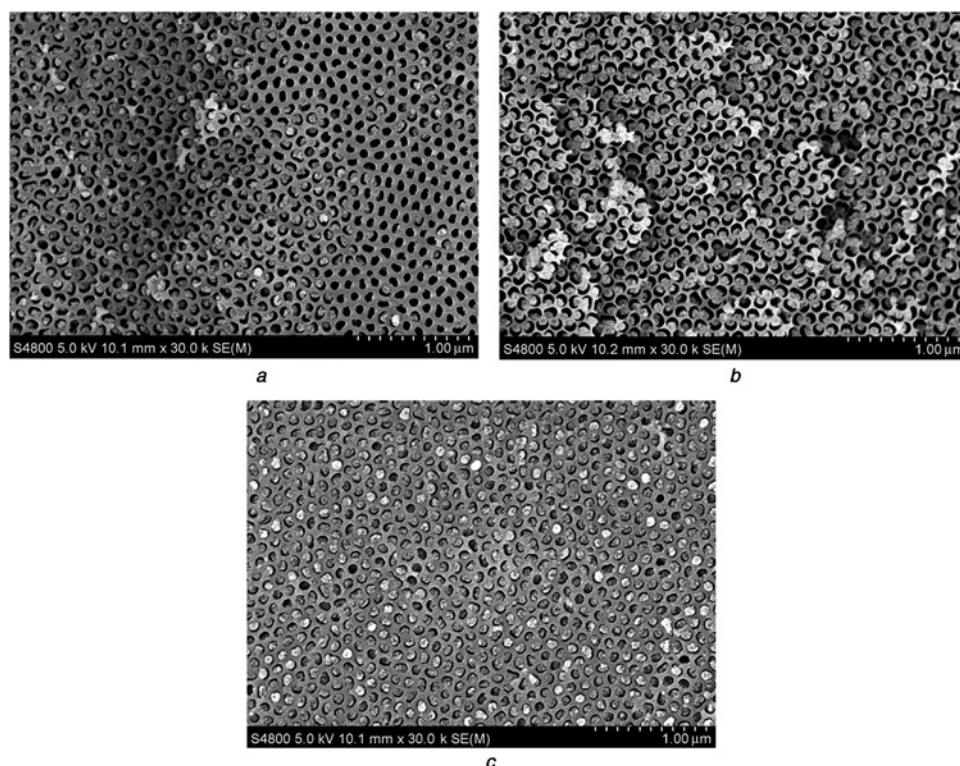


Figure 1 SEM images from top view of $\text{La}_x\text{Zn}_y\text{O}_z$ nanostructure with AAO template obtained from different reaction times
a 15 min
b 30 min
c 60 min

inset of Fig. 2. We can see a number of tiny nanoparticles closely packed to form the nanowire with a dense structure. Fig. 3 is the XRD pattern of $\text{La}_x\text{Zn}_y\text{O}_z$ nanowire arrays, in which no specific characteristic peaks relevant to the phase composition were found. Fig. 4 is the energy-dispersive X-ray spectroscopy (EDS) spectrum of $\text{La}_x\text{Zn}_y\text{O}_z$ nanowire arrays, and the results certify that the nanowire is composed of lanthanum (La), zinc (Zn) and oxygen (O) elements. The higher peak of aluminium (Al) is from the AAO, and the composition of oxygen is non-stoichiometric, which is partly contributed by the AAO.

According to the above results, 0.1 M NaOH and the mixed nitrate solution consisting of 0.01 M $\text{La}(\text{NO}_3)_3$ and 0.01 M $\text{Zn}(\text{NO}_3)_2$ were alternately dropped on the surface of the AAO template. They passed through the nanopore of the AAO template under the action of subatmospheric pressure, and a few of them stayed in the pore wall of the AAO template due to the Coanda effect. The $\text{La}_x\text{Zn}_y(\text{OH})_n$ nanowire precursor was then formed by successive co-precipitation reaction until the solution could not pass

through the porous channel of the AAO template. The total reaction time was about 60 min. Finally, the amorphous $\text{La}_x\text{Zn}_y\text{O}_z$ nanowire arrays were obtained by high-temperature decomposition of the

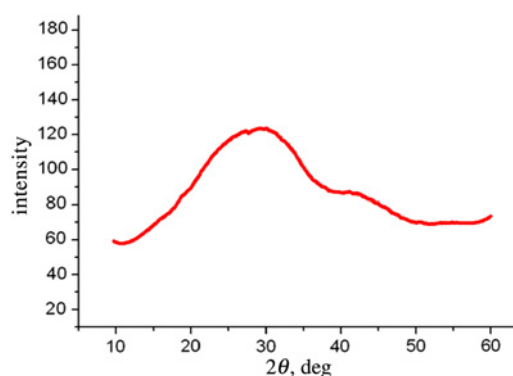


Figure 3 XRD pattern of $\text{La}_x\text{Zn}_y\text{O}_z$ nanowire arrays

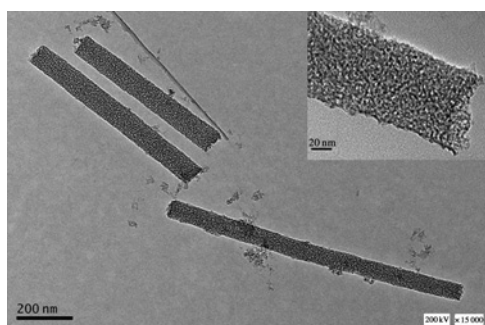


Figure 2 TEM image of $\text{La}_x\text{Zn}_y\text{O}_z$ nanowires, the inset is a high-magnification image

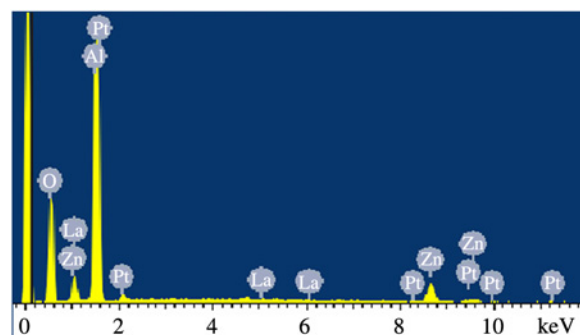


Figure 4 EDS spectra of $\text{La}_x\text{Zn}_y\text{O}_z$ nanowire arrays

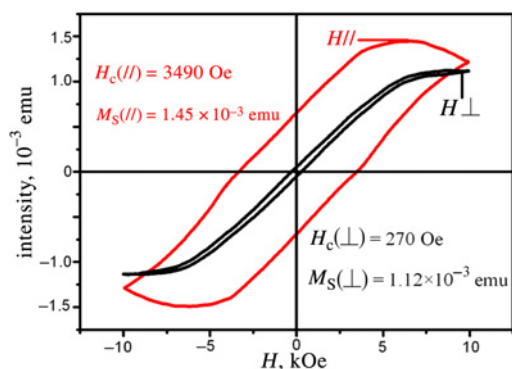


Figure 5 M - H hysteresis loops of $\text{La}_x\text{Zn}_y\text{O}_z$ nanowire arrays

hydroxide precursor. To investigate the growth process of the nanowires, the SPSF-assisted successive precipitation reaction time was decreased to 30 and 15 min.

By comparing the surface morphology of incomplete or well-aligned nanowires produced at different total reaction times, we can propose the growth process of $\text{La}_x\text{Zn}_y\text{O}_z$ nanowire arrays. First, the nanoparticles of hydroxide precursor slowly attached the wall of the partial nanopores in the AAO template from the bottom-up to form long and slim nanowires when the reaction time is 15 min. Secondly, with the reaction time increasing to 30 min, the nanowires with a minor diameter have grown on the wall of all nanopores. Lastly, the widespread and perfect $\text{La}_x\text{Zn}_y\text{O}_z$ nanowire arrays with the AAO template were fabricated when the total reaction time was increased to 60 min.

The hysteresis loops of $\text{La}_x\text{Zn}_y\text{O}_z$ nanowire arrays were measured by VSM at room temperature (Fig. 5). The applied magnetic field is parallel ($H//$) or perpendicular ($H\perp$) to the axis of the nanowire arrays. The coercive force for $H_c(H//)$ is 3490 Oe, $H_c(H\perp)$ is 270 Oe. The saturation magnetisation $M_s(H//)$ is 1.45×10^{-3} emu when the applied magnetic field of parallel ($H//$) is 6550 Oe, and the $M_s(H\perp)$ is 1.12×10^{-3} emu at ($H\perp$) 8620 Oe. This indicates that the easily magnetised direction of $\text{La}_x\text{Zn}_y\text{O}_z$ nanowire arrays is parallel to the axis of the nanowire arrays. To sum up the above data from hysteresis loops, the higher coercive force ratio of $H_c(H//)/H_c(H\perp)$ is about 13, and the saturation magnetisation in the direction of perpendicular $M_s(H\perp)$ slightly lower than parallel $M_s(H//)$ to the axis of nanowire arrays indicates obvious magnetic anisotropy behaviour in $\text{La}_x\text{Zn}_y\text{O}_z$ nanowire arrays, which is ascribed to the shape anisotropy. The magnetic anisotropy of $\text{La}_x\text{Zn}_y\text{O}_z$ nanowire arrays may determine its potential applications in ultra-high-density magnetic memory material.

4. Conclusion: Amorphous $\text{La}_x\text{Zn}_y\text{O}_z$ nanowire arrays have been fabricated by chemical co-precipitation under SPSF in the AAO template. We propose the growth process of $\text{La}_x\text{Zn}_y\text{O}_z$ nanowire arrays according to the graded surface morphology of $\text{La}_x\text{Zn}_y\text{O}_z$

nanostuctures with the AAO template fabricated at different co-precipitation reaction times of 15, 30 and 60 min. There is obvious magnetic anisotropy behaviour in $\text{La}_x\text{Zn}_y\text{O}_z$ nanowire arrays, which is attributed to the shape anisotropy.

5. Acknowledgments: This work was supported by the General Administration of Quality Supervision, Inspection and Quarantine of the People's Republic of China (2010IK079, 2012Ik-84) and the Scientific Research Plan Projects of Anhui Province Education Bureau (Kj 2011 A004).

6 References

- [1] Özgür Ü., Alivov Y.I., Liu C., *ET AL.*: 'A comprehensive review of ZnO materials and devices', *J. Appl. Phys.*, 2005, **98**, pp. 041301
- [2] Djuricic A.B., Chen X.Y., Leung Y.H., *ET AL.*: 'ZnO nanostructures: growth, properties and applications', *J. Mater. Chem.*, 2012, **22**, pp. 6526–6535
- [3] Özgür Ü., Hofstetter D., Morkoc H.: 'ZnO devices and applications: a review of current status and future prospects', *Proc. IEEE*, 2010, **98**, pp. 1255–1268
- [4] Arya S.K., Saha S., Ramirez-Vick J.E., *ET AL.*: 'Recent advances in ZnO nanostructures and thin films for biosensor applications: review', *Anal. Chim. Acta*, 2012, **737**, pp. 1–21
- [5] Sánchez F.A.L., Takimi A.S., Rodembusch F.S., *ET AL.*: 'Photocatalytic activity of nanoneedles, nanospheres, and polyhedral shaped ZnO powders in organic dye degradation processes', *J. Alloys Compd.*, 2013, **572**, pp. 68–73
- [6] Park W.: 'Controlled synthesis and properties of ZnO nanostructures grown by metalorganic chemical vapor deposition: a review', *Met. Mater. Int.*, 2008, **14**, pp. 659–665
- [7] Zacharias M., Subannajui K., Menzel A., *ET AL.*: 'ZnO nanowire arrays – pattern generation, growth and applications', *Phys. Status Solidi B*, 2010, **247**, pp. 2305–2314
- [8] Gonzalez-Valls I., Lira-Cantu M.: 'Vertically-aligned nanostructures of ZnO for excitonic solar cells: a review', *Energy Environ. Sci.*, 2009, **2**, pp. 19–34
- [9] Khatamian M., Khandar A.A., Divbanda B., *ET AL.*: 'Heterogeneous photocatalytic degradation of 4-nitrophenol in aqueous suspension by Ln (La^{3+} , Nd^{3+} or Sm^{3+}) doped ZnO nanoparticles', *J. Mol. Catal. A, Chem.*, 2012, **365**, pp. 120–127
- [10] He J.Q., Yin J., Liu D., *ET AL.*: 'Enhanced acetone gas-sensing performance of La_2O_3 -doped flowerlike ZnO structure composed of nanorods', *Sens. Actuator B, Chem.*, 2013, **182**, pp. 170–175
- [11] Jia T., Wang W.M., Long F., *ET AL.*: 'Fabrication, characterization and photocatalytic activity of La-doped ZnO Nanowires', *J. Alloys Compd.*, 2009, **484**, pp. 410–415
- [12] Suwanboon S., Amornpitoksuk P., Bangrak P., *ET AL.*: 'Structural, optical and antibacterial properties of nanocrystalline $\text{Zn}_{1-x}\text{La}_x\text{O}$ compound semiconductor', *Mater. Sci. Semicond. Process.*, 2013, **16**, pp. 504–512
- [13] Lan W., Liu Y.P., Zhang M., *ET AL.*: 'Structural and optical properties of La-doped ZnO films prepared by magnetron sputtering', *Mater. Lett.*, 2007, **61**, pp. 2262–2265
- [14] Bouznit Y., Beggah Y., Ynineb F.: 'Sprayed lanthanum doped zinc oxide thin films', *Appl. Surf. Sci.*, 2012, **258**, pp. 2967–2971
- [15] Young S.L., Chen H.Z., Kao M.C., *ET AL.*: 'Magnetic properties of La-doped and Cu-doped ZnO nanowires fabricated by hydrothermal method', *Int. J. Mod. Phys. B*, 2013, **27**, pp. 1362006